ORIGINAL PAPER

Impact of land-use change on soil erosion in the Coonoor Watershed, Nilgiris Mountain Range, Tamil Nadu, India

Subbarayan Saravanan[1] · Jesudasan Jacinth Jennifer[1] · Leelambar Singh[1] · Saranya Thiyagarajan[1] ·
Sivaranjani Sankaralingam[2]

Abstract
The conversion of native forest to the tea plantation and cropland has intensified throughout the Coonoor watershed of the Nilgiris region over the past few decades. The current study investigates the severity of land cover changes including deforestation activities in the Coonoor watershed region as a result of urbanization, along with the establishment of recreational parks, resorts and tea plantations. In order to analyse the changes, a widely used soil erosion model say Revised Universal Soil Loss Equation (RUSLE) is opted to estimate the average soil loss. Therefore, this work marks the impact of land-use changes on land degradation and the consequent vital natural phenomenon like soil erosion. The change detection was carried out for over 14 years period from 2005 to 2018. Landsat images of corresponding years were classified using the supervised classification technique. The C-factor (cover and management factor) for the corresponding periods were also identified. Conversion of forest land into tea plantations, wastelands and settlements significantly decrease the soil organic matter (SOM) and hydraulic conductivity (HC) of the soil, which leads to a difference in the K-factor (soil erodibility factor) throughout the study period, whereas the R-factor (rainfall and runoff factor) and LS-factor (length-slope factor) were considered to be constant throughout the period. Results indicate the annual soil loss during the period from 2000 to 2018 on each land use/cover classes. viz., tea plantations, 223.26 km^2; settlement, 163.35 km^2; open forest, 799.02 km^2; dense forest, 1158.48 km^2; and barren land, 27.18 km^2. The total sediment yield in the study area was found to have oddly increased due to the land use/cover changes. The significant rise of soil erosion was found evitable in the deforested region which was converted to infrastructure and wasteland.

Keywords Soil loss · RUSLE · Erosion prediction · Remote sensing · Coonoor watershed · Nilgiris · India

✉ Subbarayan Saravanan
  ssaravann@nitt.edu

  Jesudasan Jacinth Jennifer
  jacijenni36@gmail.com

  Leelambar Singh
  leeli.singh@gmail.com

  Saranya Thiyagarajan
  saranyame2205@gmail.com

  Sivaranjani Sankaralingam
  saranjanisiva@gmail.com

[1] Department of Civil Engineering, National Institute of Technology, Tiruchirappalli, India

[2] Department of Geography, Bharathidasan University, Tiruchirappalli, India

Introduction

Soil loss is a natural phenomenon, which is influenced by different factors such as land-use, elevation and other climatic factors. Over the last four decades, about one-third of the agricultural land is said to be vulnerable to soil erosion at the rate of 10 million ha per year (Sun et al. 2014). Soil erosion is caused due to wind, water, rain, surface flow, subsurface flow, coastal erosion and gravity erosion. The total soil loss in India was assessed to be 15 ton/ha/year (Sankar et al. 2018). Indian Council of Agricultural Research (ICAR) reports that about 53 Mega-hectares of soil loss occurs annually due to water. In Nilgiris, potato is one of the major crops in steep slopes, and this crop does no support to soil fixture, which ends up being a terrible cause for inducing soil erosion at the start of intense rainfall (June-September) and flooding in the low lying areas.

Nilgiris contributes 26% of the total green tea produced in India, which is another notable one that indicates the induced soil erosion activity in this plantations area.

Soil loss model is based on the empirical equations, initiated from the Universal Soil Loss Equation (Wischmeier and Smith 1978). RUSLE model is developed to quantify the soil loss for any scenario with varying crop pattern, current erosion minimising practices and management techniques (Jahun et al. 2015). Soil erosion becomes a concern as regular rate increases; this is caused due to improper agricultural practices, anthropogenic operations, extreme deforestation and inadequate infrastructure arrangements (Dregne 1987; Crosson 1997; Morgan 2009; Wantzen and Mol 2013). The management of economic balance in developing countries is balanced by extraction of the soil and land resources, which promotes deforestations and leads to wild changes in the land-use/land-cover pattern (Smith et al. 2016). One of the root causes of landslides in this region is soil disintegration. It is necessary to manage soil erosion by altering the patterns of land-use so that the rate of erosion can be controlled (Pradhan et al. 2012). Besides, changes in both climate and land-use variables have risen in previous decades due to global changes in agricultural strategies and markets. (Boardman and Favis-Mortlock 1993; Nearing et al. 2004; Simonneaux et al. 2015; Pierce and Lal 2017; Borrelli et al. 2017; Mukherjee and Singh 2020). India is one of the developing countries where most of the topsoil loss is due to erosion, which is the result of land-use changes that have increased the sediment transport rates, which now has become an environmental bane (Ahmad 1973; Dregne 1992; Kothyari and Singh 1996; Bhattacharyya et al. 2015). Erosion from reservoir siltation is an off-site effect which is severe than water pollution that spoils the land resources. Siltation affects the life of the reservoir and hydroelectricity power stations. It also affects soil fertility and crop productivity economically (Ismail and Ravichandran 2008). Soil erosion can accelerate the water retention of the soil, thereby affecting the runoff in rivers. Soil erosion also affects topography, by causing an increase in the slope gradient. Plant roots have been put under the light, as it has become a leading factor that retards the soil erosion through root exudation; plant canopy is used in measuring the impact of vegetation on water erosion (Poesen 2018).

Remote sensing techniques aids in the spatial and temporal analysis of soil erosion and the off-site effects are studied through modelling (Bahadur 2009; Tadesse et al. 2017; Uddin et al. 2018). It is important to control the soil erosion, its effect and its loss capacity (mass); hence, RUSLE model predicts the soil loss by multiplying the rainfall erosivity (R), length of slope and steepness of slope (LS), erodibility factor of soil (K), practice cover (P) and cover management factor (C). Estimating the soil loss from the RUSLE model has quite a lot of limitations concerning reliability, cost and representation. RUSLE model uses remote sensing techniques and geographical information system (GIS) tools to assess the soil loss at a reasonable cost and precisely over a large-scale region (Jain and Kothyari 2000; Jain et al. 2001; Fu et al. 2005; Bhattarai and Dutta 2007and Galdino et al. 2016). Change in the socioeconomic status of the Coonoor watershed (Nilgiris district) is primarily due to massive deforestation since the twentieth century, vast areas of mature forest have been transformed into agricultural land, pastures and wasteland (Jha et al. 2000). Another major cause of fast urbanization in the region is the influence of tourism. Geological Survey of India has projected that the cause for landslide and soil erosion was due to the development on the slopes.

Hence, here is an approach to examine the critical zone which requires control measures and the need to be addressed in long-term planning. The underlying objective of this research is to compute the loss of soil due to erosion in different Land-use classes using geospatial techniques and study the rate of increase in erosion over the decades from 2000 to 2018.

Study area

Coonoor watershed is located in the Nilgiris district of Tamil Nadu, India (Figure 1). It lies between the latitude 11°20'0" N and 11°25'0"N and longitude 76°44'0"E and 76°50'0" E. Topography of the study area is hilly and steep, varying from 1500 to 2546 m elevation from MSL. Doddabetta, which lies in this district is the highest peak in Southern India with an elevation of 2595 m above the mean sea level. Other notable hills of this district include Devarshola peak, Hulical hill, Elk hills and Cairn hill. Plenty of waterfalls exist here and, notably, a stream flows between every pair of mountains. The most remarkable streams among them are Pykara that originates from the slopes of the Peak Mukkuruthi. This region receives its maximum rainfall during the southwest monsoon (June-September) and the annual average rainfall of the Nilgiris district remains from 1400 to 2000 mm/year. The soil texture of the study area could be classified as loamy and clay-loam. The Coonoor Municipality has a population of 45,494 and the region is comprised of 22% of forest area. This region is vulnerable to landslides and has a history of decades of landslides (Jaiswal et al. 2011; Saravanan et al. 2010 and Chandrasekaran et al. 2013a. The most predominant bedrock material is Charnockite, overlain with laterite, which forms an irregular soil horizon. The rocks are metamorphic in nature, and various geomorphic features comprised in this region are Debris slope, Denudational Hill, Denudational Slope, Plateau. The economy of this region highly depends on the cultivation of tea plantations. The temperature of the district ranges between 18 and 28 °C during summer and between 0 and 16 °C during winter. The soil gets saturated even during low-intensity rains and water flush through the fissures rapidly.
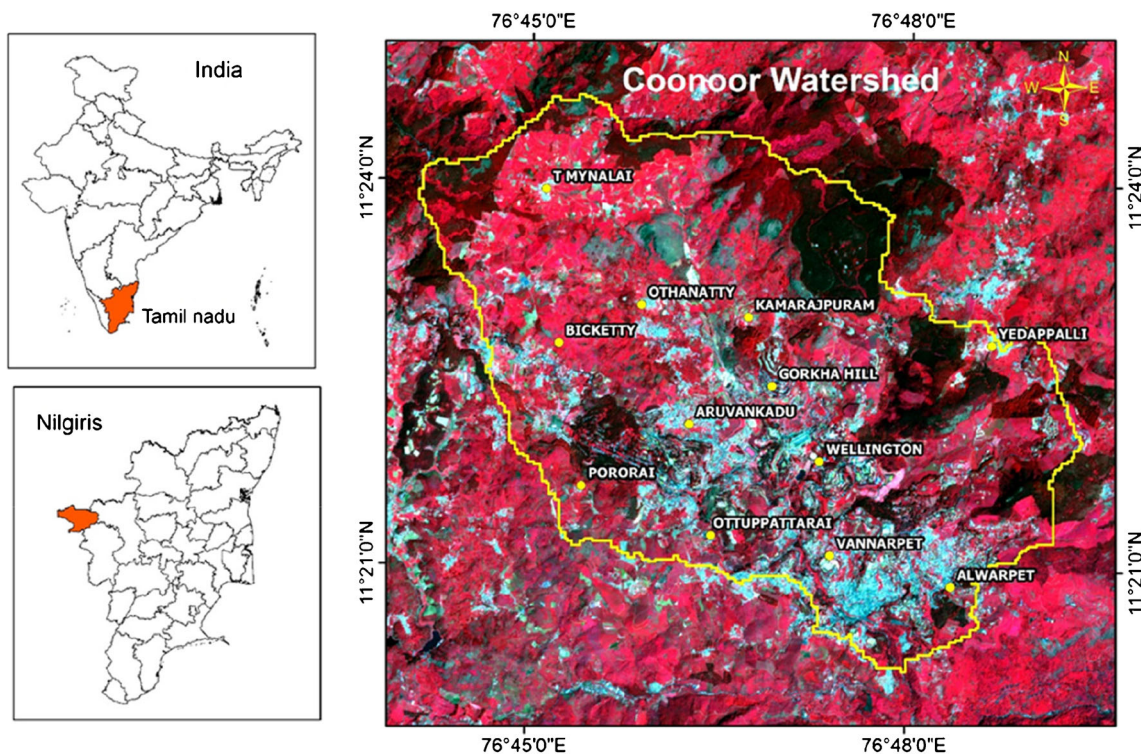
Figure 1 Map showing the location of the Coonoor watershed

Material and methods

To evaluate soil erosion, firstly satellite data were administered to radiometric corrections to generate a quality image from the satellite data. These data are further processed to generate accurate Land-use (LU) and Land-cover (LC) maps. Radiometric correction is a combination of several procedures prescribed to change the digital numbers to real reflectance (Pons et al. 2014). Landsat 8 OLI and Landsat 5 TM satellite imagery (Path 144, Row 52) were downloaded from the United States Geological Survey (USGS) portal (https://earthexplorer.usgs.gov/). These Landsat images have a revisit period of 16 days and a spatial resolution of 30 m.

There are many methods available to estimate soil erosion of the watershed such as Empirical models which can be applied with sufficient ease, because of their simplified structures and reliability like Stehlik Model, Erosion Potential Method (EPM), Bureau of Land Management (BLM), Food and Agriculture Organization (FAO) Model, Scalogram Model, Geoland 2, Ephemeral Gully Erosion Model (EGEM), Musgrave Model, Soil-Loss Estimation for Southern Africa (SLEMSA), Universal Soil-Loss Equation (USLE), Revised Universal Soil-Loss Equation (RUSLE) and Erosion Productivity Impact Calculator (EPIC) Pacific-Southwest Inter-agency Committee (PSIAC) (Fakhri et al. 2014; Jiao et al. 2018). The RUSLE parameters are commonly used for agricultural and forest area average annual soil loss estimation. In this research, Revised Universal Soil Loss Equation (RUSLE) is applied to determine and quantify the soil erosion (Millward and Mersey 1999; Xu et al. 2019). This model has been used over the years for its simple structure, and it is the updated type of soil-loss estimation compared with USLE (Wischmeier and Smith 1965). RUSLE is a widely applicable model and allows more flexibility in estimating soil losses (Sinha and Joshi 2012; Pan and Wen 2014; Pham et al. 2018; Fayas et al. 2019). It is a grouping of process-based and experimental designs thus hold benefit over the USLE concerning maximum usage of the database. Flow chart explains the process involved in deriving the factors from various sources for estimating soil erosion (Fig. 2).

The fundamental equation for soil erosion estimation is:

$$A = R*K*LS*C*P \tag{1}$$

where A is the soil loss (tonnes/hectare), R factor is the rainfall-runoff erosivity (MJ- mm/ ha/ h), K factor represents the soil erodibility (ton/ha/h/MJ/mm), S factor is the steepness of slope, L factor is the length-of-slope, P factor is the support and conservation practices and C factor is the cover/management.

The methodology adopted in this research was the application of the RUSLE model using GIS techniques. Survey of India (SOI) toposheets were used for delineating the boundary of the watershed. For the model, soil texture map from National Bureau of Soil Survey and Land Utilisation Planning (NBSS & LUP) and satellite images were used.
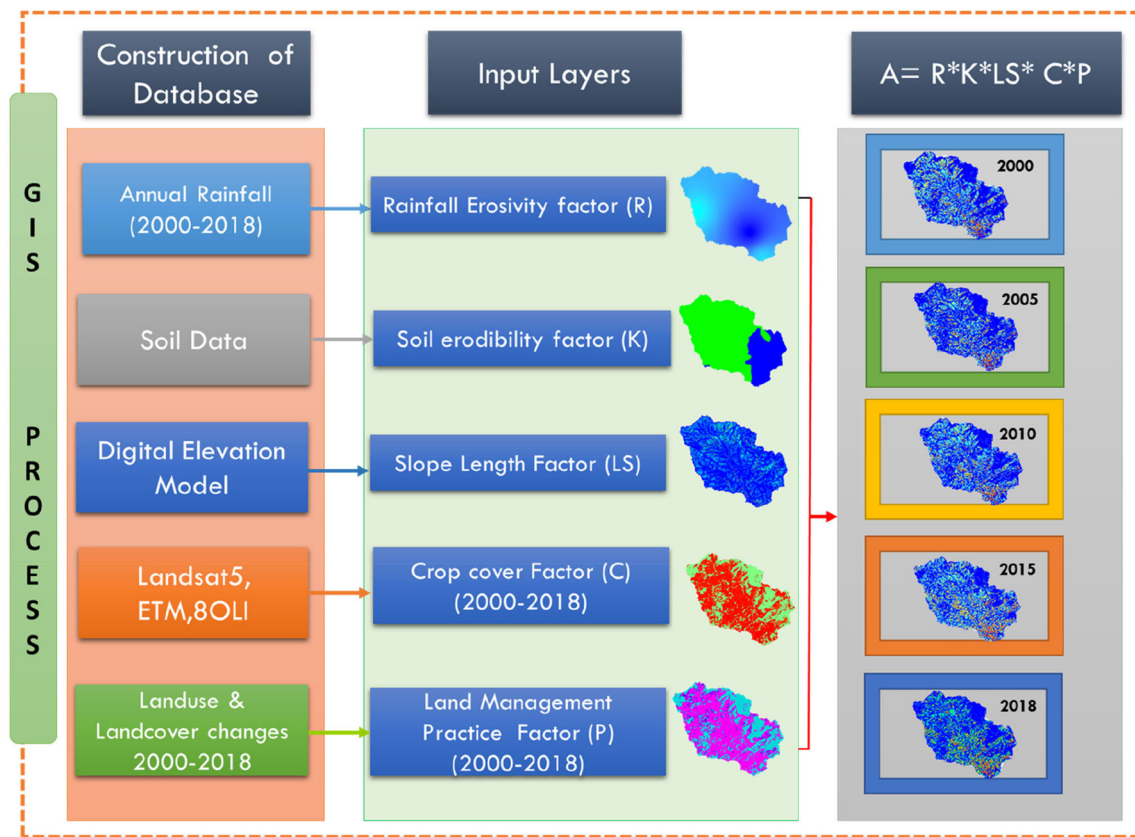
Figure 2 Methodology Flowchart

Terrain and climatic factors from the meteorological department of India (IMD) were procured.

Results and discussion

Estimating the potential area of soil erosion is necessary for sustainable agricultural and management planning. The spatially distributed soil loss mapping was derived using the five-factor, viz., R factor, rainfall erosivity; LS factor, slope-length and slope-steepness factor; P factor, supportive-practice; C factor, cover-management; and K factor, soil erodibility. All factors are incorporated in the RULSE model (Eq. 1) for the years 2000, 2005, 2010, 2015 and 2018 to evaluate soil loss.

Image processing and accuracy assessment

Remote sensing (RS) data is a primary source for studying the spatial and temporal variability of land use and land cover changes. Radiometric corrections (RC) process was used to calibrate the digital number to satellite reflectance, and it was classified into two types, viz., absolute and relative. Radiometric corrections were applied to the satellite images of five different years (2000, 2005, 2010, 2015 and 2018) to

remove the anomaly due to solar illumination, scattering and absorption. Dark object subtraction (DOS) adopts the features in the imagery that have zero reflectance from atmospheric scattering. In each band, the DOS looks for the darkest pixel value and subtract that value from all bands thus effectively removing haze in multispectral data.

Land-use and Land-cover analysis

Remote sensing and GIS-based Land Use/Land Cover (LULC) analysis help in understanding the changes in the environment that have occurred. False colour composite (FCC) was used for a viewing the multispectral image. This FCC band combinations enhance the images, enabling the identification the LULC classes effectively. The vegetation in found in shades of red, water in dark blue and settlements in cyan blue. In this study, the supervised classification technique was adopted and the digital image is classified based on the maximum likelihood algorithm (Otukei and Blaschke 2010). Level 1 classification proposed by Anderson was adopted (Anderson et al. 1976). The study area was primarily classified into five classes of barren land, settlement, tea, dense forest and open forest (Fig. 3), and the changes were analysed (Fig. 4). Settlement class follows an increasing trend
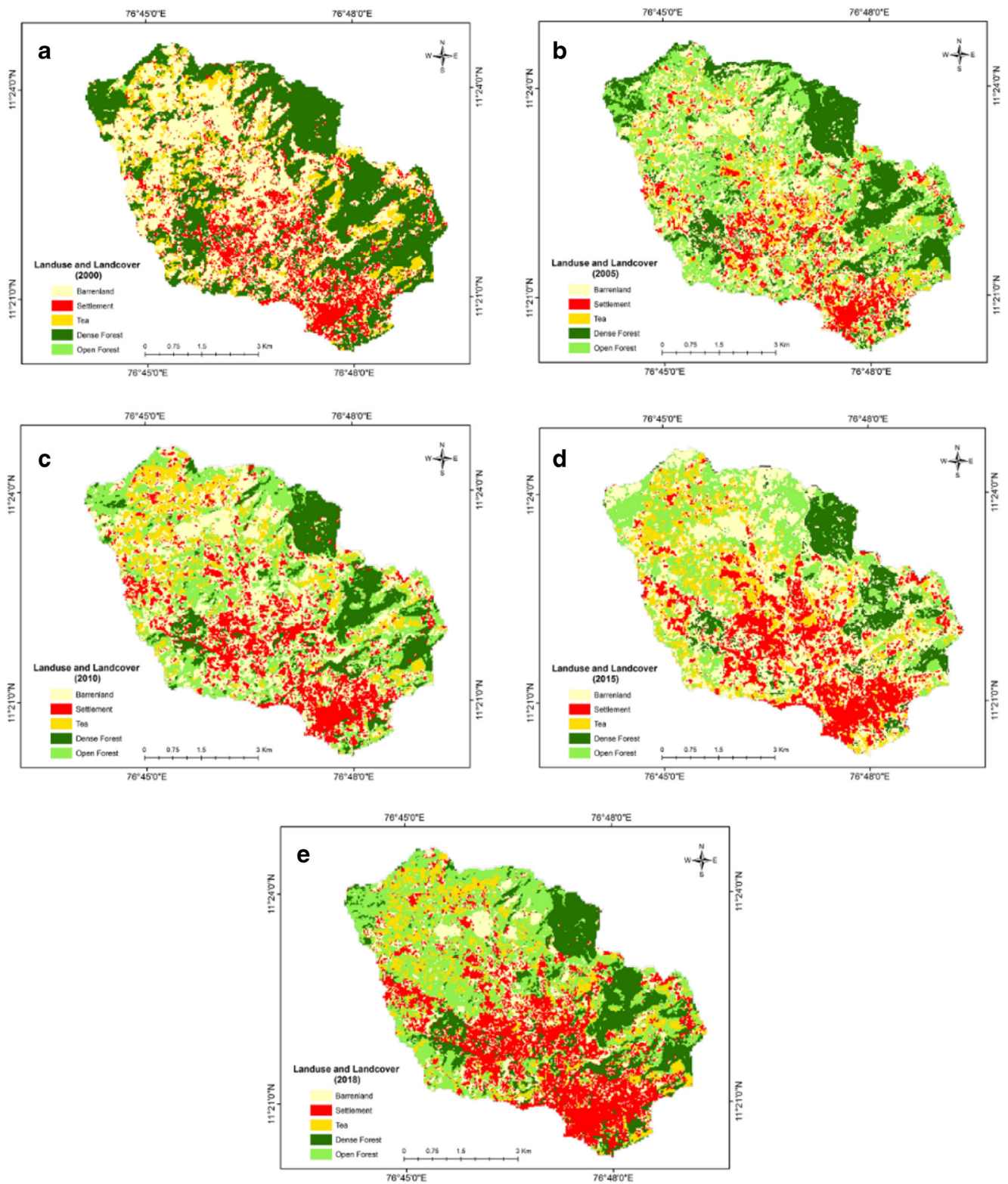
Figure 3 Land use and land cover map-2000-2018

followed by tea plantation; this tract of the trend-line could be due to the increasing urbanization which is directly proportional due to the population growth (Pathak et al. 2020) .

Accuracy assessment is essential for LU/LC, to ascertain its quality and uncertainty (Czaplewski and Patterson 2003). The possible errors in the LULC may be due to data

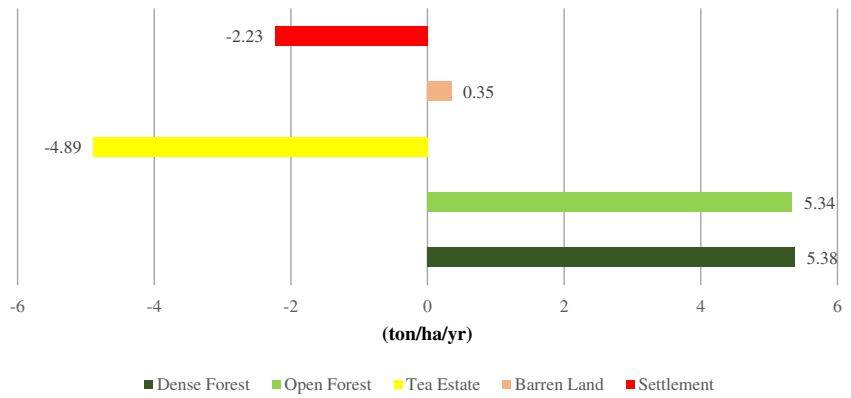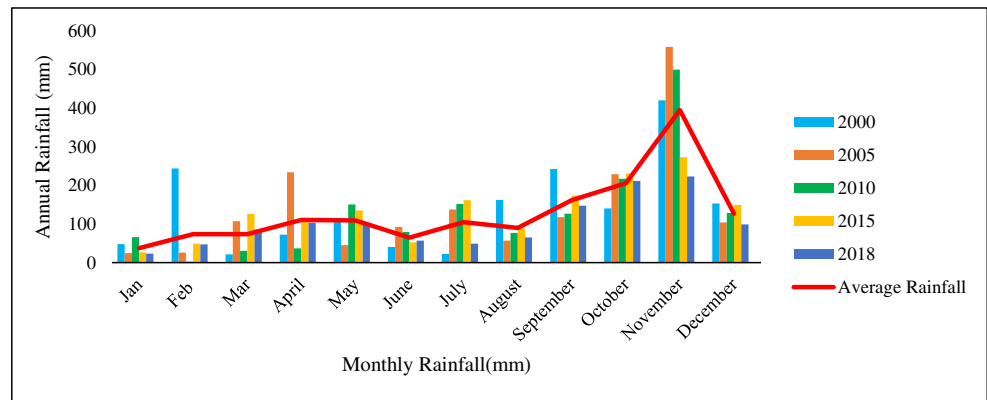**Figure 4** Land use and land cover changes

Figure 5 Long term average Annual Rainfall

misclassification. There are two common methods for accuracy assessment. First one is omission error where producer's accuracy is based on the specific LULC feature on the ground to check whether it is classified as the same in the image (ratio of classified pixels to the total number of the pixel). In the user's accuracy,

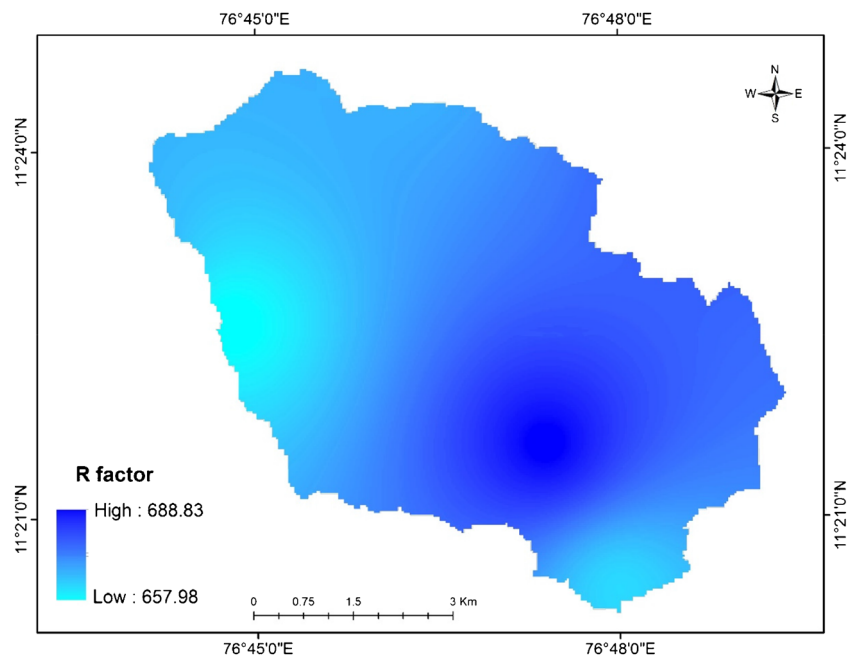**Figure 6** Rainfall erosivity factor

Table 1 K factor value of soil texture

Soil texture	Organic carbon content	K factor
Clay loam	1.1	0.274
Loam	1.3	0.371

the error of omission is measured by the percentage of LULC feature pixels on the map to the corresponding ground (Shao and Wu 2008; Paolini et al. 2006). Classification accuracy has been assessed using the recent dataset as a reference, random pixels were selected, and for each pixel, the land use accuracy was assessed using the kappa coefficient. The obtained Kappa coefficient of the land use in this study was 0.7, 0.76, 0.71, 0.78 and 0.81 for the years 2000, 2005, 2010, 2015 and 2018, respectivaly. According to LULC 2000, there was 25.39% dense forest, 48.12% open forest, 12.39% tea estate, 9.22% barren land and 4.88% settlement, whereas in 2018 it has changed into 12.32% dense forest, 37% open forest, 28.40 tea estate, 9.22% barren land and 12.09% settlement that indicates a prominent hike in the establishments of the settlement in the region indicating a rapid increase in the urbanization between the years 2000 and 2018.

Rainfall erosivity (R)

This index was derived to measure the erosive force of rainfall. R is a function of intensity, duration and

volume of rainfall. Increase in the intensity and quantity of rainfall causes an increase in the R-value. This factor greatly reflects the rill and sheet erosion caused due to rainfall (Smith and Wischmeier 1957; Cerdan et al. 2006). The erosive potential of the soil is higher as a result of rainfall intensity and duration. Annual rainfall data were obtained for the respective years (2000, 2005, 2010, 2015 and 2018) (Fig. 5) from the Tamil Nadu meteorological department and were spatially interpolated to generate the annual rainfall intensity map. It has been used for quantifying the intensity of rainfall and its erosivity. R-factor was computed based on the following expression:

$$R = \left[4.17\left(\frac{p_i 2}{P}\right) - 152\right] \qquad (2)$$

where R factor represents the erosivity (MJ mm ha-1 year-1), P is the mean annual rainfall in mm and P_i is the mean monthly rainfall in mm. The R-factor map was synthesised using the IDW interpolation techniques in ArcGIS software (Fig. 6).

The graph of rainfall shows annual rainfall and has an average rainfall of 1551 mm. November 2015 has recorded a maximum rainfall with a 555.1 mm. The elevated area is struck with erosion due to heavy rainfall. R-factor values help in estimating rainfall erosivity and, areas, which are at high risk comparing the soil erodibility, cover-management factor and supportive-practice factor slope-length and slope-steepness factor.

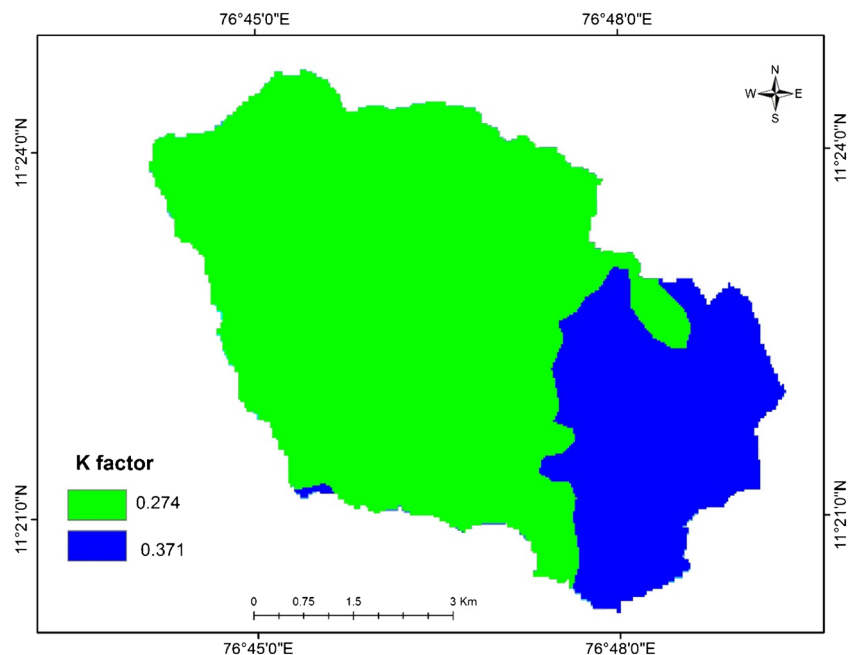**Figure 7** Map showing the spatial variation of K-factor

Table 2 Crop-management factor (C) value for various LU-LC classes

| LULC classes	C factor value	Source
Settlement	1	Biswas et al., (2015)
Barren land	0.18	Pandey et al. (2007) and Biswas et al., (2015)
Tea	0.16	Kartic et al. (2014)
Dense forest	0.003	Andrade et al. (2010)
Open forest	0.013	Andrade et al. (2010)

K-factor

The tendency of the soil getting eroded provides a measure of soil loss, which is detached by external forces. It is the conjunctional consequence of rainfall, soil infiltration and surface runoff (Renard et al. 1997). Soil erodibility can be classified with reference to soil texture. Fieldwork to assess soil erodibility is time-consuming. Thus, soil data prepared by the Indian Council of Agricultural Research-NBSS & LUP is exploited in this study. Soil erodibility can be identified according to soil class, soil texture and organic matter. The equivalent value of K is assigned with reference to different studies (Bonilla and Johnson 2012; Biswas and Pani 2015). The K factor was assigned based on the different soil texture (Table 1), and the map was generated using ArcGIS software (Fig. 7). Following equation was used to compute the K factor (3) (Wischmeier. et.al 1978).

$$100K = 2.713M^{1.14}(10^{-4})(12-a) + 3.25(b-2)$$
$$+ 2.5(c-3) \tag{3}$$

where 'M' expresses the effect of topsoil texture and is calculated as (% silt + % sand) *(100% - % clay), 'a' is the topsoil organic matter (%), 'b' is class of topsoil structural code and 'c' is the soil permeability class code.

Length of slope and slope steepness factor (LS)

The topographical aspect plays a crucial part in soil erosion model. The slope length influences the sediment yield and the amount of steepness; thus it is accounted for the model. The steepness of the slope influences the runoff (Thomaz 2009) and thereby soil loss (Liu et al. 2000). Computation of the LS factor requires the flow accumulation and slope data and are generated from the digital elevation model (DEM) using the ArcGIS software (Fig. 8). LS was computed with the basic equation that follows (Moore and Burch 1986):

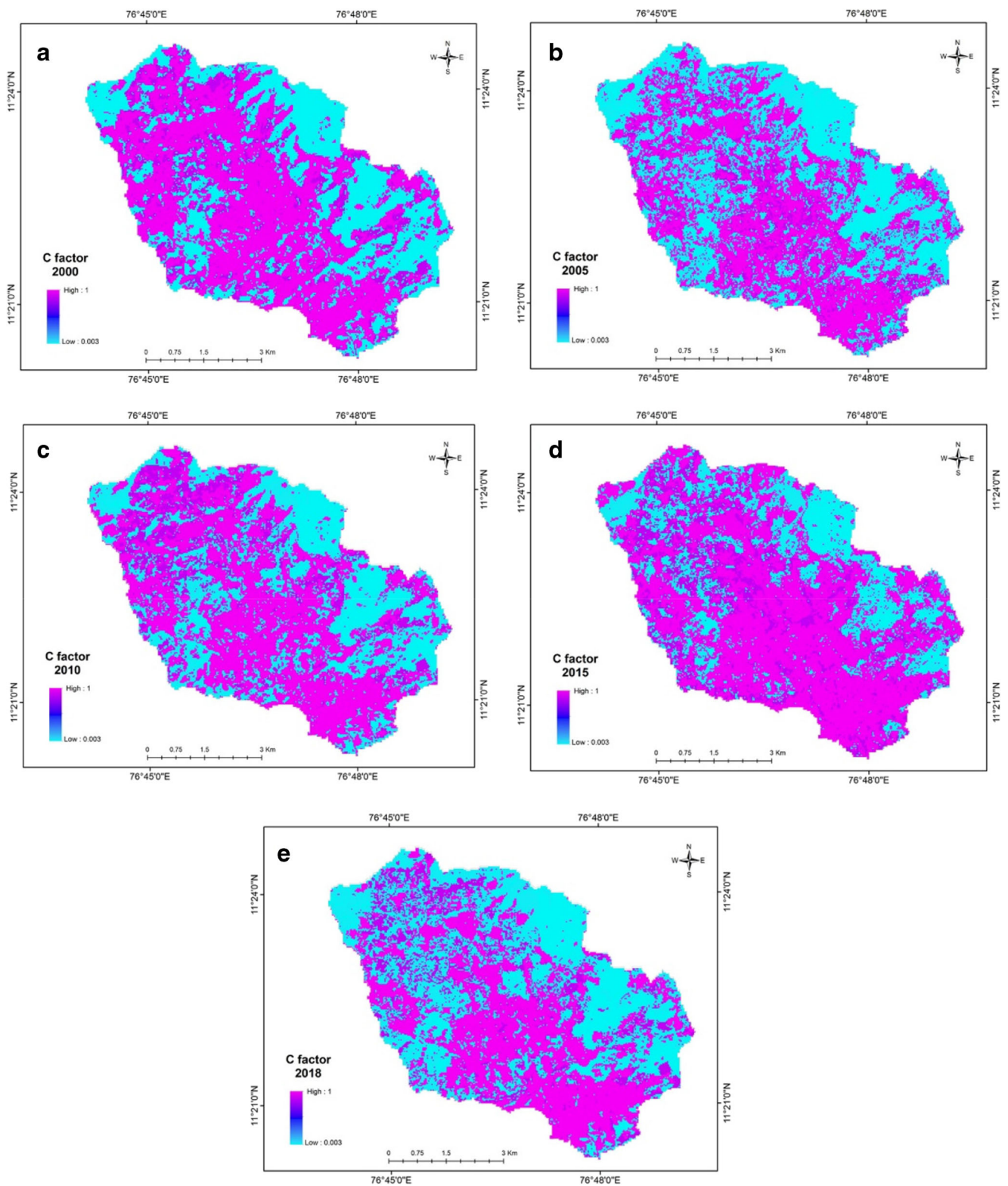**Figure 9** Crop Management factor (C) of Coonoor watershed
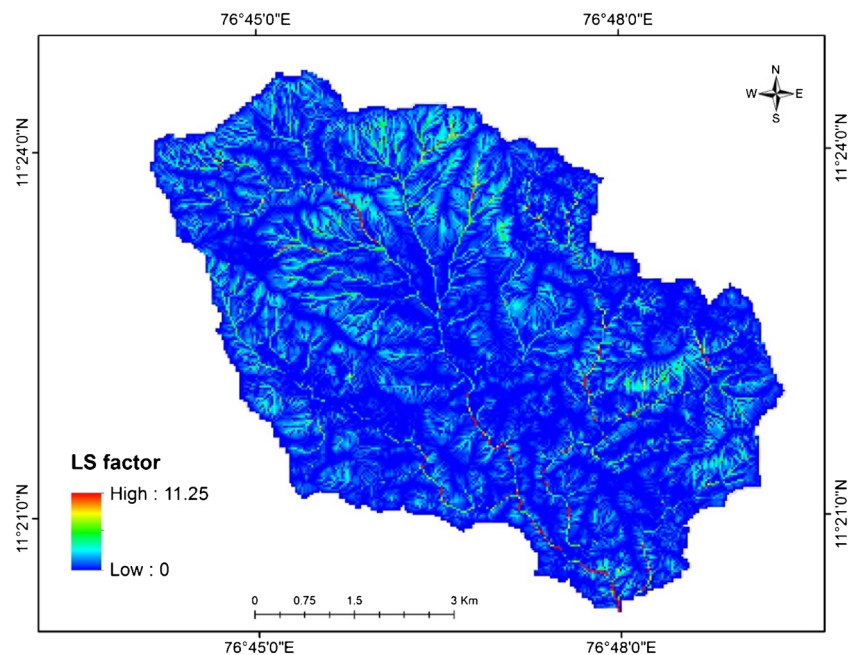
Figure 10 Support practice (P) factor of Coonoor watershed

$$LS = (Flow\_accumulation \times Cellsize/22.13)^{0.4}$$
$$\times (\sin slope/0.089)^{1.3} \qquad (3)$$

In which, the flow accumulation represents the flow accumulated upslope contributing area for a cell. LS being the integrated slope-length and slope-steepness factor, the analysis based on Eq. (3) was performed

Table 3 The area under the soil loss class of Coonoor watershed

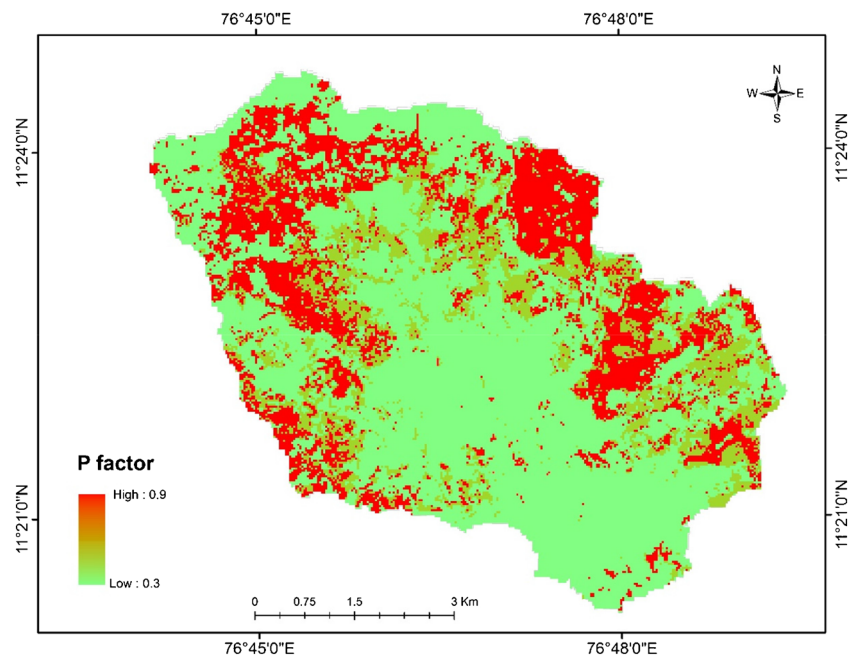| LULC	2000 (km²)	2005 (km²)	2010 (km²)	2015 (km²)	2018 (km²)
Tea	441.72	411.03	516.51	566.55	665.01
Settlement	709.56	515.52	788.13	1136.43	872.91
Open forest	38.97	1212.75	1118.16	1327.05	837.99
Dense forest	1623.96	920.88	670.32	814.05	465.48
Barren land	1710	1458.54	1431.09	680.13	1682.82

using raster calculator in ArcGIS and LS factor is found to range from 0 to 11.25.

Figure 8 spatially distributed map of Slope-length and steepness-factor

Crop management (C) and support practice (P) factor

Crop-management factor (C) describes the ratio of soil loss due to change in cropland and management practices (Pandey et al. 2007). Vegetated areas reduce the effect of soil erosion by increasing infiltration and reducing rainfall energy. Remote sensing data is the best source of C-factor estimation as it is possible to distinguish various land-use trends for temporal use (Uddin et al. 2016). The value of C-factor is based on its vulnerability, such that, the land-use with the highest value is said to be highly sensitive to soil erosion and vice versa. Thus, values of C-factor in the study area were found to vary from 0.003 for the dense forest to 1 for settlement.

Crop cover controls erosion and nutrient leaching, protects seedling and is strongly related to soil water runoff properties (Unger and Vigil 1998). The C-factor values were derived from land-use and land-cover (LULC) classes of the watershed (Table 2). The LULC maps of the year 2000, 2005, 2010, 2015 and 2018 (Fig. 9) were prepared from the Landsat satellite image. Supportive factor (P) reflect the rate and amount of runoff, which reduces erosion. P-factor is the soil erosion divided by specific practice factor. Generally, P-factor value varies between 0 and 1 and in this research and were assigned based on the land-use class and slope (Wischmeier and Smith 1978; Abdurachman et al. 1984; Xu et al. 2013). The maximum values of P-factor, 1 were given to settlement and 0.18 to barren land, while the minimum values were given to dense forest and open forest as 0.003 and 0.013 respectively (Fig. 10)

The sensitivity analysis implies the rate of soil erosion controlled using cover management factor (C) and LS factor (LS) which are deemed to be critical due to the severity in the rainfall intensity. Raster calculator tool in GIS software was used to calculate the contribution of respective factor, and the final maps were generated for the following years: 2000, 2005, 2010, 2015 and 2018.

Estimation of soil erosion potential

The erosion potential of Coonoor watershed was performed using the RUSLE model using ArcGIS 10.4 Software. The potential soil erosion map was categorized into 5 Land-use classes tea, settlement, open forest, dense forest, barren land with the corresponding resultant potential soil erosion map of the years 2000 (Fig. 11), 2005 (Fig. 12), 2010 (Fig. 13), 2015

Figure 11 Soil erosion potential of Coonoor, 2000

Figure 12 Soil erosion potential
of Coonoor, 2005
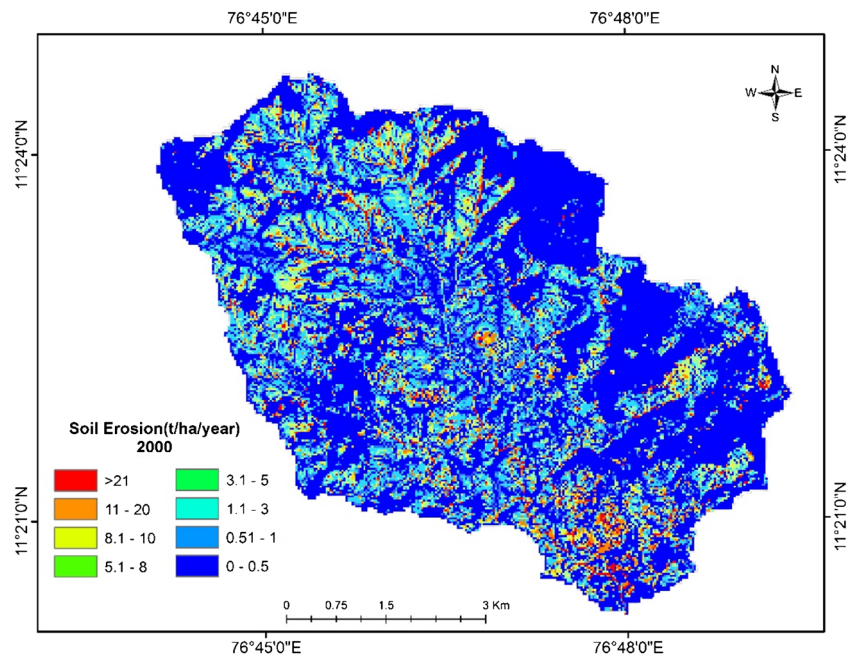
(Fig. 14) and 2018 (Fig. 15). The results imply that the settlement region located on lower elevated terrain in the southern portion of the study area is highly influenced by soil erosion, and area over 163km^2 was found to be affected from 2000 to 2018, while the northeast region was found to be the less affected area. Tea was found to be the most vulnerable entity for soil erosion, tea planters converted forest area into tea for over 224 km^2 area which has effected the soil erosion from 2000 to 2018. The drastic erosion can be witnessed in the years 2015–2018 as about 100 km^2 of the region underwent erosion. Meanwhile, the dense forest has changed to open

forest and barren land for over 1000 km^2, and there shows a decrease in the negative social process for cultivation. However, from the resultant map of the year 2018 (Fig. 14), it was observed that the southern region, as well as northern region, was highly vulnerable to soil erosion, though the southern region is claimed to be the highly affected zone. In this scenario, the northeast part was found to be less affected. During the study period, the expected annual average soil loss risen by 16%, between 2000 and 2018, respectively. From resultant maps, the percentage increase in area for the critical class (>20(t/ha)) was found to be 1.3, 1.5, 1.6, 1.4 and 2.3 for

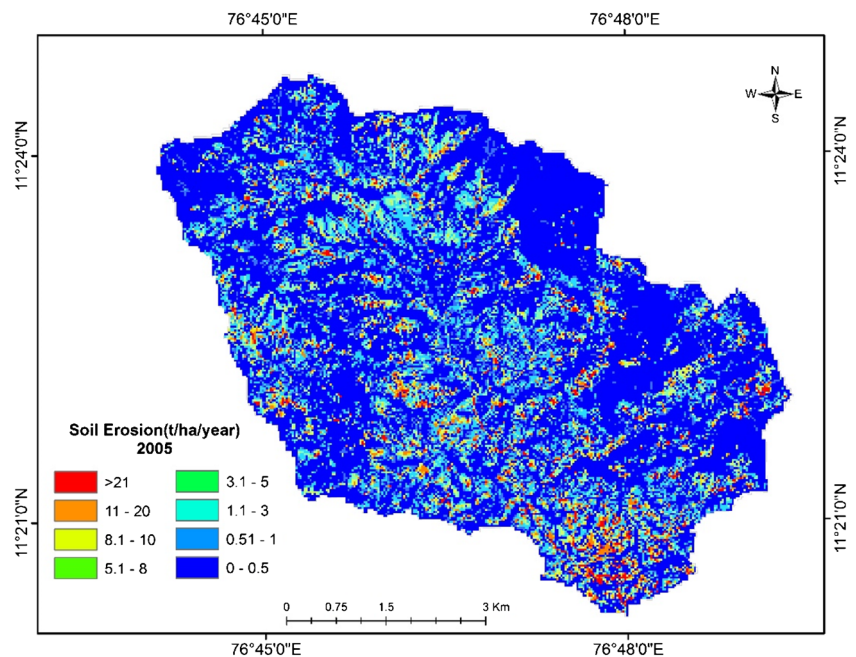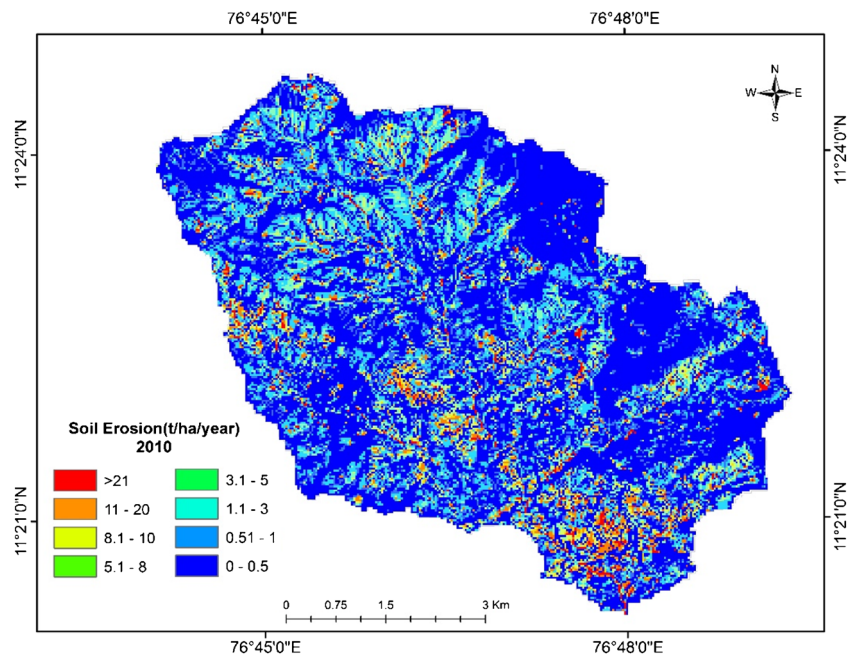**Figure 13** Soil erosion potential
of Coonoor, 2010

Figure 14 Soil erosion potential of Coonoor, 2015

the years 2000, 2005, 2010, 2015 and 2018, respectively. As specified in Table 3, the most vulnerable region with high soil erosion has been found increasing over the years from 2000 to 2018 with respect to specific land-use classes. In the years 2000–2005, the rate of change was less when compared with the years 2010–2015 as the open forest is changed to a tea plantation. Heavy rainfall occurred in 2009 and triggered landslides which is the major reason for high erosion in 2010. The erosion rate declined in 2015, which may also be associated with the change in the land use pattern in 2018, and the erosion rate was very high and was found increased by

2.13%; this increment in erosion rate is proportional to the increase in settlement and tea plantation over the years. The slope between > 7 and ≤ 13 was found to be critical, which has an upward trend of soil erosion over the years from 2000 to 2018. The percentage of the area which falls under the slope class of > 7 and ≤ 13 are 29.03, 35.74, 55.24, 59.51 and 59.62% for the corresponding years of 2000, 2005, 2010, 2015 and 2018. From the land-use pattern and steepness of the terrain, the potential soil erosion of the region has been analysed spatially and temporally. There are also similar variations in the forest cover, from dense to open forest, and it

Figure 15 Soil erosion potential of Coonoor, 2018
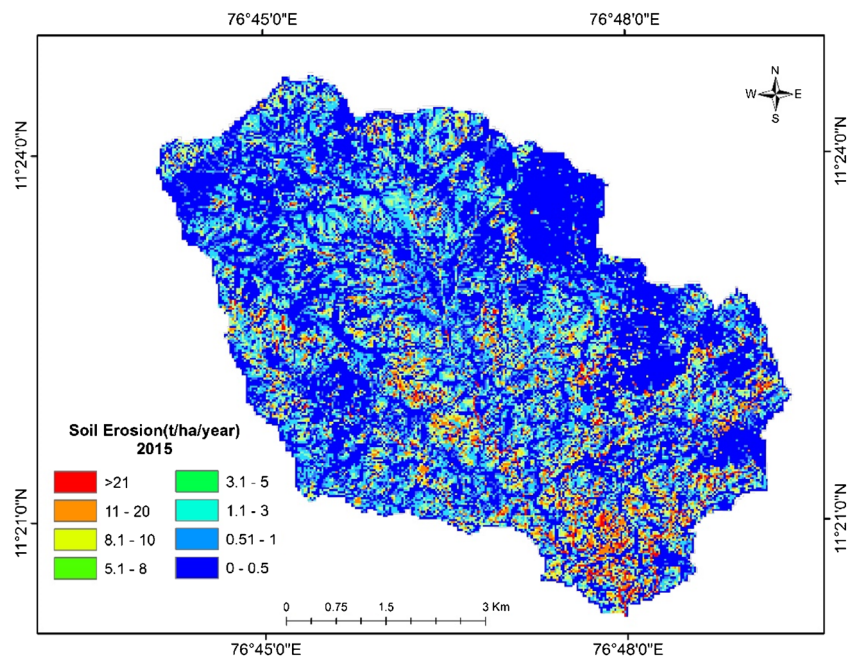
activates the vulnerability; deforestation has highly promoted erosion. High rainfall zones also contribute to the erosion in the barren land. Population stress in urbanization is another factor inducing erosion. Therefore, soil conservation practices should be implemented focussing on proper agricultural practices, soil infiltration, reducing the steep slope and proper diversion of stormwater to reduce the runoff.

Conclusion

This research highlights the soil erosion estimation under different land-use scenarios for the years from 2000 to 2018. Estimation of soil erosion has been carried out by using the RUSLE model combined with the remote sensing and GIS techniques. These estimates imply that 70% region of the Coonoor watershed falls under moderate soil loss class (< 5 t/ha/year). However, under different land-use scenarios, the degree of soil loss class was in increasing trend. Spatial analysis indicates that both the southern and northern region of the study area was under severe soil loss, and this scenario could be due to severe terrain modification and raw agricultural practices in those regions, along with the conjunctional influence of LS-factor, K-factor and also C-factor. The fallow lands remain highly susceptible to erosion followed by the tea and other plantation crops, which have replaced the natural forests. With the change in LULC pattern, the slope of the terrain is also disturbed, thereby loosening the topsoil layer inducing erosion. Other reasons which considerably increased the soil loss are the broadening of road slopes, which reduces the soil shear strength at the toe; improper drainage maintenance caused by blockages and the infiltration into slopes caused mass landslides (Chandrasekaran et al. 2013b). Based on the results, the slope being > 7, ≤ 13 and > 26 were highly susceptible to erosion activity. The erosion can be reduced by proper management practices; crop rotation over gazing should be stopped. Likewise, the government also should promote technological development to put bring out methods to hinder and mitigate the erosion, stabilisation of slopes and plantation of *Vetiveria zizanioides (Vetiver grass)* which when planted in rows across the slope holds the soil tight preventing it from erosion.

Declarations

Conflict of interest The authors declare that they have no conflict of interest.

References

Abdurachman A, Abuyamin S, Kurnia U (1984) Pengelolaan Tanah dan Tanaman untuk Usaha Konser vasi (Soil and Crop Management for Conservation Enterprises), Pusat Penelitian Tanah Bogor. In: Asdak C (ed) Hidrologi dan Pengelolaan Daerah Aliran Sungai (Hydrology and Watershed Management). Gajah Mada University Press, Yogyakarta, pp 371–374

Ahmad E (1973) Soil erosion in India. Asia Publishing House

Anderson JR, Hardy EE, Roach JT, & Witmer RE (1976). A land use and land cover classification system for use with remote sensor data. USGS Professional Paper 964. US Geological Survey, 28

Andrade O, Kappas M, Erasmi S (2010) Assessment of erosion hazard in Torres municipality of Lara State (Venezuela) based on GIS. Interciencia 35(5):348–356

Bahadur KK (2009) Mapping soil erosion susceptibility using remote sensing and GIS: a case of the Upper Nam Wa Watershed, Nan Province, Thailand. Environ Geol 57(3):695–705

Bhattacharyya R, Ghosh B, Mishra P, Mandal B, Rao C, Sarkar D, Franzluebbers A (2015) Soil degradation in India: challenges and potential solutions. Sustainability 7(4):3528–3570

Bhattarai R, Dutta D (2007) Estimation of soil erosion and sediment yield using GIS at catchment scale. Water Resour Manag 21(10): 1635–1647

Biswas SS, Pani P (2015) Estimation of soil erosion using RUSLE and GIS techniques: a case study of Barakar River basin, Jharkhand, India. Model Earth Syst Environ 1(4):42

Boardman J, Favis-Mortlock DT (1993) Climate change and soil erosion in Britain. Geogr J 159:179–183

Bonilla CA, Johnson OI (2012) Soil erodibility mapping and its correlation with soil properties in Central Chile. Geoderma 189:116–123

Borrelli P, Robinson DA, Fleischer LR, Lugato E, Ballabio C, Alewell, C.,& Bagarello, V. (2017) An assessment of the global impact of 21st century land use change on soil erosion. Nat Commun 8(1): 2013

Cerdan O, Poesen J, Govers G, Saby N, Le Bissonnais Y, Gobin A, Kwaad FF (2006) Sheet and rill erosion. Soil Erosion Europe:501–513

Chandrasekaran SS, Elayaraja S, Renugadevi S (2013a) Damages to Transport Facilities by Rainfall Induced Landslides During November 2009 in Nilgiris, India. In: Damages to transport facilities by rainfall induced landslides during November 2009 in Nilgiris, India, In Landslide Science and Practice (pp. 171-176). Springer, Berlin, Heidelberg

Chandrasekaran SS, Owaise RS, Ashwin S, Jain RM, Prasanth S, Venugopalan RB (2013b) Investigation on infrastructural damages by rainfall-induced landslides during November 2009 in Nilgiris, India. Nat Hazards 65(3):1535–1557

Crosson P (1997) Will erosion threaten agricultural productivity? Environ Sci Policy Sustain Dev 39(8):4–31

Czaplewski RL, Patterson PL (2003) Classification accuracy for stratification with remotely sensed data. For Sci 49(3):402–408

Dregne HE (1987) Soil erosion: cause and effect. Land Use Policy 4(4): 412–418

Dregne HE (1992) Erosion and soil productivity in Asia. J Soil Water Conserv 47(1):8–13

Fakhri M, Dokohaki H, Eslamian S, Fazeli Farsani I, Farzaneh MR (2014) Flow and sediment transport modeling in rivers. Handb Eng Hydrol 2:233–275

Fayas CM, Abeysingha NS, Nirmanee KGS, Samaratunga D, Mallawatantri A (2019) Soil loss estimation using rusle model to prioritize erosion control in KELANI river basin in Sri Lanka. Int Soil Water Conserv Res 7(2):130–137

Fu BJ, Zhao WW, Chen LD, Zhang QJ, Lü YH, Gulinck H, Poesen J (2005) Assessment of soil erosion at large watershed scale using RUSLE and GIS: a case study in the Loess Plateau of China. Land Degrad Dev 16(1):73–85

Galdino S, Sano EE, Andrade RG, Grego CR, Nogueira SF, Bragantini C, Flosi AH (2016) Large-scale modeling of soil erosion with RUSLE for conservationist planning of degraded cultivated Brazilian pastures. Land Degrad Dev 27(3):773–784

Ismail J, Ravichandran S (2008) RUSLE2 model application for soil erosion assessment using remote sensing and GIS. Water Resour Manag 22(1):83–102

Jahun BG, Ibrahim R, Dlamini NS, Musa SM (2015) Review of soil erosion assessment using RUSLE model and GIS. J Biol Agric Health 5(9)

Jain MK, Kothyari UC (2000) Estimation of soil erosion and sediment yield using GIS. Hydrol Sci J 45(5):771–786

Jain SK, Kumar S, Varghese J (2001) Estimation of soil erosion for a Himalayan watershed using GIS technique. Water Resour Manag 15(1):41–54

Jaiswal P, Van Westen CJ, Jetten V (2011) Quantitative estimation of landslide risk from rapid debris slides on natural slopes in the Nilgiri hills, India. Nat Hazards Earth Syst Sci 11(6): 1723–1743

Jha CS, Dutt CBS, Bawa KS (2000) Deforestation and land use changes in Western Ghats. India Curr Sci:231–238

Jiao P, Yu Y, & Xu D (2018). Evaluation of EPIC model on predicting runoff, soil erosion, and nitrate and dissolved phosphorus loss. In 2018 ASABE Annual International Meeting (p. 1). American Society of Agricultural and Biological Engineers

Kartic KM, Annadurai R, Ravichandran PT (2014) Assessment of soil erosion susceptibility in Kothagiri Taluk using revised universal soil loss equation (RUSLE) and geo-spatial technology. Int J Sci Res Publ 4(10):1–13

Kothyari UC, Singh VP (1996) Rainfall and temperature trends in India. Hydrol Process 10(3):357–372

Liu BY, Nearing MA, Shi PJ, Jia ZW (2000) Slope length effects on soil loss for steep slopes. Soil Sci Soc Am J 64(5):1759–1763

Millward AA, Mersey JE (1999) Adapting the RUSLE to model soil erosion potential in a mountainous tropical watershed. Catena 38(2):109–129

Moore ID, Burch GJ (1986) Modelling erosion and deposition: topographic effects. Trans ASAE 29(6):1624–1630

Morgan RPC (2009). Soil erosion and conservation. John Wiley & Sons

Mukherjee F, Singh D (2020) Assessing land use–land cover change and its impact on land surface temperature using LANDSAT data: A comparison of two urban areas in India. Earth Syst Environ 4(2): 385–407

Nearing MA, Pruski FF, O'neal MR (2004) Expected climate change impacts on soil erosion rates: a review. J Soil Water Conserv 59(1):43–50

Otukei JR, Blaschke T (2010) Land cover change assessment using decision trees, support vector machines and maximum likelihood classification algorithms. Int J Appl Earth Obs Geoinf 12: S27–S31

Pan J, Wen Y (2014) Estimation of soil erosion using RUSLE in Caijiamiao watershed, China. Nat Hazards 71(3):2187–2205

Pandey A, Chowdary VM, Mal BC (2007) Identification of critical erosion prone areas in the small agricultural watershed using USLE, GIS and remote sensing. Water Resour Manag 21(4): 729–746

Paolini L, Grings F, Sobrino JA, Jiménez Muñoz JC, Karszenbaum H (2006) Radiometric correction effects in Landsat multi-date/multi-sensor change detection studies. Int J Remote Sens 27(4): 685–704

Pathak C, Chandra S, Maurya G, Rathore A, Sarif MO, Gupta RD (2020) The effects of land indices on thermal state in surface urban heat island formation: a case study on Agra City in India using remote sensing data (1992–2019). Earth Syst Environ:1–20

Pham TG, Degener J, Kappas M (2018) Integrated universal soil loss equation (USLE) and Geographical Information System (GIS) for soil erosion estimation in A Sap basin: Central Vietnam. Int Soil Water Conserv Res 6(2):99–110

Pierce FJ, & Lal R (2017). Monitoring the impact of soil erosion on crop productivity. In Soil erosion research methods(pp. 235-263). Routledge

Poesen J (2018) Soil erosion in the Anthropocene: Research needs. Earth Surf Process Landf 43(1):64–84

Pons X, Pesquer L, Cristóbal J, González-Guerrero O (2014) Automatic and improved radiometric correction of Landsat imagery using reference values from MODIS surface reflectance images. Int J Appl Earth Obs Geoinf 33:243–254

Pradhan B, Chaudhari A, Adinarayana J, Buchroithner MF (2012) Soil erosion assessment and its correlation with landslide events using remote sensing data and GIS: a case study at Penang Island, Malaysia. Environ Monit Assess 184(2):715–727

Renard KG, Foster GR, Weesies GA, McCool DK, Yoder DC (1997) Predicting soil erosion by water: a guide to conservation planning with the Revised Universal Soil Loss Equation (RUSLE), vol 703. United States Department of Agriculture, Washington

Sankar M, Green SM, Mishra PK, Snöälv JTC, Sharma NK, Karthikeyan K, Thilagam VK (2018) Nationwide soil erosion assessment in India using radioisotope tracers 137Cs and 210Pb: the need for fallout mapping. Curr Sci 115(3):388

Saravanan S, Sathiyamurthi S, Elayaraja D (2010) Soil erosion mapping of Katteri watershed using universal soil loss equation and geographic information system. J Indian Soc Soil Sci 58(4):418

Shao G, Wu J (2008) On the accuracy of landscape pattern analysis using remote sensing data. Landsc Ecol 23(5):505–511

Simonneaux V, Cheggour A, Deschamps C, Mouillot F, Cerdan O, Le Bissonnais Y (2015) Land use and climate change effects on soil erosion in a semi-arid mountainous watershed (High Atlas, Morocco). J Arid Environ 122:64–75

Sinha D, Joshi VU (2012) Application of universal soil loss equation (USLE) to recently reclaimed badlands along the Adula and Mahalungi Rivers, Pravara Basin, Maharashtra. J Geol Soc India 80(3):341–350

Smith DD, Wischmeier WH (1957) Factors affecting sheet and rill erosion. EOS Trans Am Geophys Union 38(6):889–896

Smith P, House JI, Bustamante M, Sobocká J, Harper R, Pan G, West PC, Clark JM, Adhya T, Rumpel C, Paustian K, Kuikman P, Cotrufo MF, Elliott JA, McDowell R, Griffiths RI, Asakawa S, Bondeau A, Jain AK, Meersmans J, Pugh TA (2016) Global change pressures on soils from land use and management. Glob Chang Biol 22(3):1008–1028

Sun W, Shao Q, Liu J, Zhai J (2014) Assessing the effects of land use and topography on soil erosion on the Loess Plateau in China. Catena 121:151–163

Tadesse L, Suryabhagavan KV, Sridhar G, Legesse G (2017) Land use and land cover changes and Soil erosion in Yezat Watershed, North Western Ethiopia. Int Soil Water Conserv Res 5(2):85–94

Thomaz EL (2009) The influence of traditional steep land agricultural practices on runoff and soil loss. Agric Ecosyst Environ 130(1-2): 23–30

Uddin K, Murthy MSR, Wahid SM, Matin MA (2016) Estimation of soil erosion dynamics in the Koshi basin using GIS and remote sensing to assess priority areas for conservation. PLoS One 11(3):e0150494

Uddin K, Abdul Matin M, Maharjan S (2018) Assessment of land cover change and its impact on changes in soil erosion risk in Nepal. Sustainability 10(12):4715

Unger PW, Vigil MF (1998) Cover crop effects on soil water relationships. J Soil Water Conserv 53(3):200–207

Wantzen K, Mol J (2013) Soil erosion from agriculture and mining: a threat to tropical stream ecosystems. Agriculture 3(4):660–683

Wischmeier WH, & Smith DD (1965). Predicting rainfall erosion losses from cropland east of the Rocky Mountains, USDA Agric Handb, 282

Wischmeier WH, & Smith, DD (1978). Predicting rainfall erosion losses-a guide to conservation planning. Predicting rainfall erosion losses-a guide to conservation planning

Xu L, Xu X, Meng X (2013) Risk assessment of soil erosion in different rainfall scenarios by RUSLE model coupled with Information Diffusion Model: A case study of Bohai Rim, China. Catena 100:74–82

Xu C, Yang Z, Qian W, Chen S, Liu X, Lin W, Xiong D, Jiang M, Chang CT, Huang JC, Yang Y (2019) Runoff and soil erosion responses to rainfall and vegetation cover under various afforestation management regimes in subtropical montane forest. Land Degrad Dev 30(14): 1711–1724